

## Alignment of H(2p) following H<sup>+</sup>-He, Ar charge-changing collisions

R Hippler<sup>†</sup>, W Harbich<sup>†</sup>, M Faust<sup>†</sup>, H O Lutz<sup>†</sup> and L J Dubé<sup>‡</sup>

<sup>†</sup> Fakultät für Physik, Universität Bielefeld, D-4800 Bielefeld, Federal Republic of Germany

<sup>‡</sup> Fakultät für Physik, Universität Freiburg, D-7800 Freiburg, Federal Republic of Germany

Received 3 September 1985

**Abstract.** Experimental results for the integral alignment  $A_{20}$  of H(2p) following charge-changing collisions of protons with helium and argon atoms are presented for incident energies of 1-5 keV and 35-300 keV. In addition, theoretical calculations in the continuum-distorted-wave approximation were performed. The observed discrepancies between experiment and theory are discussed.

### 1. Introduction

Polarisation or angular correlation studies provide a powerful tool to investigate details of electronic processes in atomic collisions (for a review see Hippler 1985). We are at present following a programme to investigate electron capture processes to the H( $n = 2$ ) state by proton projectiles. The object of this work is to specify as completely as possible the states of all reaction partners involved, and thereby to draw from experiment maximum information for selected collision systems. So far only certain aspects of this problem have been elucidated; e.g. the alignment (shape) of the H( $n = 2$ ) state at proton energies below about 25 keV, either integrated (Teubner *et al* 1970) or differential (Hippler *et al* 1985) with respect to the projectile scattering angle, or the orientation (transferred angular momentum) below 5 keV proton energy (Hippler *et al* 1985).

In this paper, we want to present results on the integral alignment (i.e. integrated over the scattering angle of the projectile) of H(2p) following charge-changing collisions with helium and argon targets over an extended proton energy range. In particular we have investigated the processes



for proton energies from about 0.5 to 5 keV and from 35 to 300 keV. Together with previous measurements by Teubner *et al* (1970) which cover the range 0.5-24 keV, experimental data are now available in the impact energy range 0.5-300 keV. This provides a set of data which spans the regime of molecular processes at low incident energies to the region of direct Coulomb interaction at high energies. In addition, a few measurements for deuteron impact on argon at low incident energies will be presented. The concept of alignment and orientation in atomic collisions was introduced by Macek and Jaecks (1971) and by Fano and Macek (1973). Here we define

the integral alignment  $A_{20}$  (referred to the primary beam axis) as (see, e.g., Hippler 1985)

$$A_{20} = (\sigma_1 - \sigma_0) / \sigma(2p) \quad (2)$$

where  $\sigma_0$  and  $\sigma_1$  are the partial cross sections for H(2p<sub>0</sub>) and H(2p<sub>1</sub>) excitation, respectively, and  $\sigma(2p) = \sigma_0 + 2\sigma_1$ .  $A_{20}$  is obtained from a measurement of the linear polarisation  $P$  (light observation angle 90° with respect to the incident proton direction) of the emitted Lyman- $\alpha$  radiation ( $\lambda = 121.6$  nm) following the decay of H(2p) to the H(1s) ground state,

$$P = (I_{\parallel} - I_{\perp}) / (I_{\parallel} + I_{\perp}) = (3\sigma_0 - 3\sigma_1) / (7\sigma_0 + 11\sigma_1) \quad (3)$$

where  $I_{\parallel}$  and  $I_{\perp}$  are the intensities of light with electric vector parallel and perpendicular to the incident proton direction, respectively. Thus,  $A_{20}$  is related to  $P$  by

$$A_{20} = 6P / (P - 3). \quad (4)$$

## 2. Experimental method

The measurements have been performed at two different installations. Basically, both consist of an ion accelerator, a scattering chamber and a polarisation-sensitive detector for Lyman- $\alpha$  radiation. Some details of the set-up used for the measurements at the lower energies may be found elsewhere (Hippler *et al* 1985). The experiments at the higher ion energies were performed at the Bielefeld 350 kV ion accelerator. In both measurements, proton beam currents of typically about 30 nA have been employed. The target gas was introduced into the scattering chamber through a multi-channel capillary array, resulting in a pressure enhancement in the observation region of about a factor of ten. The argon measurements were made with two background pressures of 3 and  $9 \times 10^{-5}$  mbar; for the cross section and polarisation results no significant difference at these two pressures was observed. During the helium measurements the background pressure was maintained at typically  $3 \times 10^{-4}$  mbar. No pressure dependence of the polarisation was observed when the helium pressure was raised from  $1.5 \times 10^{-4}$  mbar to  $5 \times 10^{-4}$  mbar. Lyman- $\alpha$  radiation emitted from a 2.5 cm length of ion beam containing the interaction region was detected in a polarisation-sensitive detector. This consisted of a curved suprasil mirror and a photomultiplier (EMR 542 J) having a LiF window and a KBr photocathode. The useful wavelength window of this photomultiplier ranged from 105 to 155 nm. The suprasil mirror was arranged at Brewster's angle (about 60°); it effectively transmits light with an electric vector perpendicular to the plane formed by the incident and the reflected light propagation directions. During the measurements this plane was perpendicular to the proton direction; the light observation angle was thus  $\theta_y = 90^\circ$ . The instrumental polarisation of this arrangement was measured to be 65%. A rotatable quarter-wave ( $\lambda/4$ ) plate was placed in front of the suprasil mirror. The linear polarisation  $P$  was then obtained from a measurement of the light intensity  $I(\alpha)$  at  $\alpha = 0^\circ$  and  $45^\circ$ , where  $\alpha$  is the angle between the 'fast axis' of the  $\lambda/4$  plate and the incident proton direction (Clarke and Grainger 1971):

$$P = [I(45^\circ) - I(0^\circ)] / I(45^\circ). \quad (5)$$

Typical measuring times for a polarisation measurement were between 0.1 and 10 h, during which the  $\lambda/4$  plate was rotated typically every 10 s.

### 3. Results and discussion

#### 3.1. Proton-helium collisions

Theoretical and experimental results for the integral alignment  $A_{20}$  of  $H(2p)$  in proton-helium collisions are displayed in figures 1 and 2. Our experimental data span collision energy ranges of about 0.5–5 keV and 35–300 keV; they are compared with experimental data of Teubner *et al* (1970) covering the energy range between 0.5 and 24 keV. The two data sets agree with each other in the region of overlap at low incident energies, and connect well to each other at the larger energies around 30 keV (figure 1). At low incident velocities charge exchange excitation of  $H(2p)$  is expected to proceed via couplings in the transiently formed quasi-molecule (see, e.g., Hippler 1985 and references therein). In a first step the elastic channel couples with the charge exchange channel; it is followed in a second step by radial (mainly  $2p\sigma-2s\sigma$  or  $2p\sigma-3p\sigma$ ) or rotational (mainly  $2p\sigma-2p\pi$ ) couplings with higher-lying molecular orbitals (MO). The MO in question here are  $\sigma$  and  $\pi$  states resulting in  $H(2p_0)$  and  $H(2p_1)$  final states, respectively. The small observed alignment at low incident energies indicates that both MO contribute with about equal probability to the total  $H(2p)$  excitation. Recently, Kimura and Lin (1985) have extended so-called unified AO-MO calculations to two-electron systems. In these calculations the time-dependent electronic wavefunctions are expanded in atomic orbitals (AO) or molecular orbitals (MO) at large or small internuclear separations, respectively. Their results for  $H(2p)$  charge exchange excitation in  $H^+$ -He collisions are displayed in figure 1. Excellent agreement with the experimental data is observed up to rather high proton energies. It is interesting to

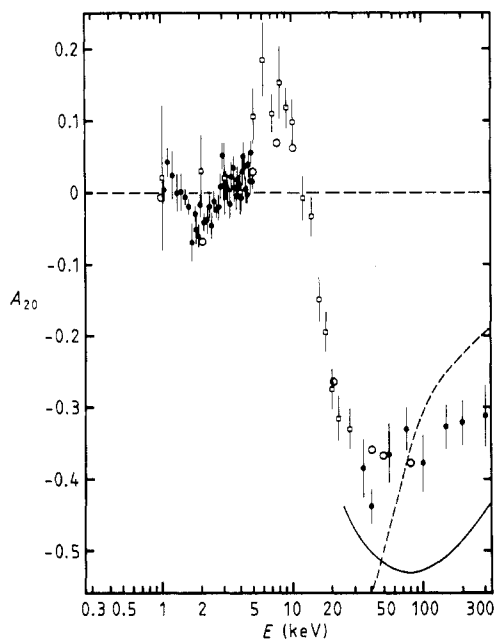


**Figure 1.** Integral alignment  $A_{20}$  plotted against incident proton energy for  $H^+$ -He collisions. Experiment: ●, present data; □, Teubner *et al* (1970); —, present CDW calculation; - - -, present CDW calculation including post-collision interaction (PCI); ○, unified AO-MO calculation (Kimura and Lin 1985).

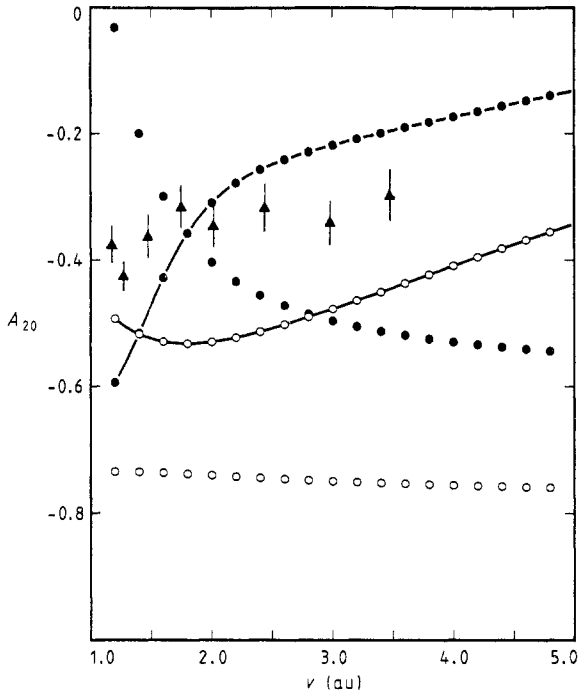


**Figure 2.** Integral alignment  $A_{20}$  plotted against incident proton velocity for  $H^+$ -He collisions. Theory:  $\text{---}\circ\text{---}$ , present CDW calculation;  $\text{---}\bullet\text{---}$ , present CDW calculation including post-collision interaction (PCI);  $\text{---}\circ\text{---}$ , first Born approximation,  $\bullet$ , first Born approximation including PCI. Experiment:  $\blacktriangle$ , present data.

note, however, that such good agreement is not observed for the total  $H(2p)$  cross section (Kimura and Lin 1985, and below).

At larger incident energies, on the other hand,  $H(2p)$  excitation results from a one-step capture process. In this collision regime, we have used the continuum distorted wave approximation (CDW, Cheshire 1964, Dubé 1984) to calculate capture cross sections together with a Hartree-Fock wavefunction to represent the He initial state. Furthermore, we have supplemented our CDW ansatz by allowing for the final-state mixing of the nearly degenerate hydrogenic levels due to the Coulombic field of the residual target ion. The inclusion of this effect has proven very important in previous studies and the reader is referred to Burgdörfer (1981) and Burgdörfer and Dubé (1984) for further details and incentives of this post-collision interaction (PCI) model.

As seen from figure 1, the CDW calculations predict large negative values of  $A_{20}$  around 100 keV ( $v = 2$  au) incident energy. These results are not inconsistent with the experimental data, but the qualitative agreement is less than satisfactory. A few remarks appear to be in order. First, the CDW approximation is a high-energy approach and for the present collision system one would not expect the theory to be valid below approximately 100 keV. Second, the CDW approach is a multiple scattering model and should provide an improvement over the first Born (B1) approximation which contains only the single scattering contribution to the capture mechanism (see, e.g., Macek 1984). To list this assertion, we have made in figure 2 a comparison between the predictions of the CDW and B1 approximations. One notices immediately the different velocity dependence of the two theories where indeed one can show that at asymptoti-

cally large velocities  $A_{20}(\text{B1}) \rightarrow -0.786$  as distinct from  $A_{20}(\text{CDW}) \rightarrow +0.125$ . Although the use of a higher-order theory improves substantially upon the B1 approximation, this can only be considered as a first step in a more adequate description of the capture process.

One should also note that the experimental data at projectile energies of 200 keV or greater have to be taken with caution. To illustrate this we have measured relative cross sections for H(2p) excitation in proton-helium collisions for incident energies from 35 to 300 keV. This was done, for a constant helium pressure, by dividing the measured signal rates from H(2p) excitation by the integrated beam current collected in a Faraday cup. The relative H(2p) excitation cross sections thus obtained were made absolute by normalisation at 70 keV to the measurements of Hughes *et al* (1970) and are displayed in figure 3. It is well known (see, e.g., Thomas 1972) that in collisions of protons with helium targets excited  $\text{He}^+$  ions are produced. In the proton energy range of interest here emission cross sections for the  $\text{He}^+ n=4 \rightarrow n=3$  transitions have

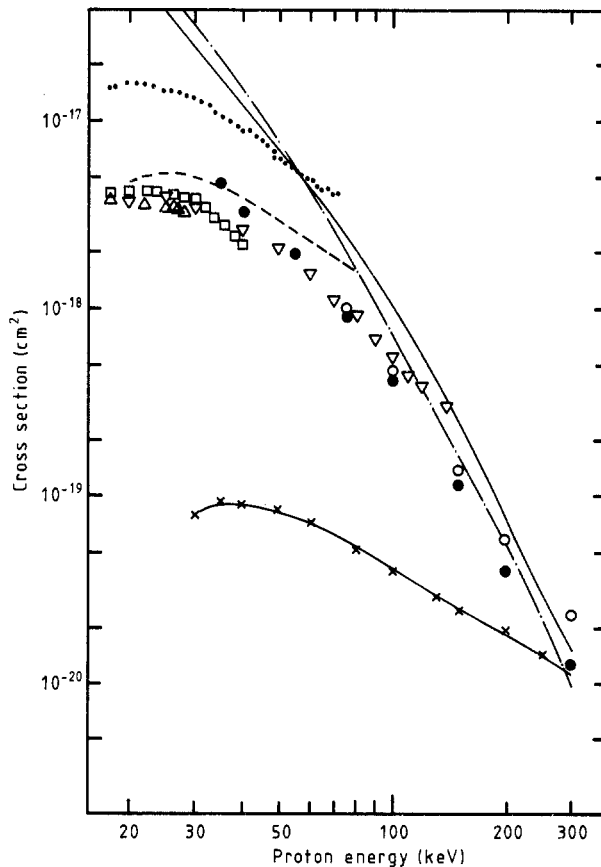


**Figure 3.** Cross sections for production of excited hydrogen atoms in proton-helium charge-changing collisions. H(2p):  $\circ$ , present results;  $\bullet$ , present results corrected for production of  $\text{He}^+(n=4)$  states;  $\bullet$ , Dose (1966);  $\triangle$ , Pretzer *et al* (1964);  $\square$ , Andreev *et al* (1966);  $\nabla$ , Hughes *et al* (1970);  $-x-$ , emission cross sections for production of line radiation from  $\text{He}^+(n=4 \rightarrow n=3)$  transitions (Moustafa Moussa and de Heer 1967, Thomas and Bent 1967, see text); present CDW calculations with  $- \cdot -$  and without  $-$  inclusion of the post-collision interaction (PCI);  $- - -$ , unified AO-MO calculations (Kimura and Lin 1985).

been measured by Moustaffa Moussa and de Heer (1967) and Thomas and Bent (1967). This transition is a measure for the production of the excited  $\text{He}^+(n=4)$  state, which may also decay to the  $n=2$  state. The  $\text{He}^+ n=4 \rightarrow n=2$  transition gives rise to emission of radiation with a wavelength of  $\lambda = 121.51$  nm, too close to that of the hydrogen Lyman- $\alpha$  radiation to be separated in our photon detector. Thus the experimental results for the helium target contain a contribution from  $\text{He}^+(n=4)$  excitation. In figure 3 the emission cross sections for the  $\text{He}^+ n=4 \rightarrow n=3$  transitions as measured by Moustaffa Moussa and de Heer (1967) and Thomas and Bent (1967) are displayed. The cross sections of Thomas and Bent (1967) were multiplied by a factor of 2.3 to join them with the measurements of Moustaffa Moussa and de Heer (1967) in the energy range of overlap. As was discussed by Hasselkamp *et al* (1971) other measurements of Thomas and Bent (1967) also appear to be too small by about the same factor. Applying averaged transition probabilities for the decay of the  $n=4$  levels to  $n=3$  and 2 respectively (*CRC Handbook of Chemistry and Physics* 1979), we infer roughly equal emission cross sections for both channels. Thus about 30% at 200 keV and 45% at 300 keV of the measured cross section are due to formation of excited  $\text{He}^+(n=4)$  states. Subtracting the  $n=4 \rightarrow n=3$  emission cross section from the measured photoemission cross section we obtain satisfactory agreement with the CDW calculations above approximately 100 keV (figure 3). Assuming the light emission from the  $\text{He}^+(n=4 \rightarrow n=2)$  transition to be unpolarised, we could now correct the  $A_{20}$  values (figure 1) accordingly. This would shift  $A_{20}$  to larger negative values at the highest proton energies: the correction would be negligible up to 150 keV, and would reach about 30% at 200 keV. Clearly, this correction would not improve the agreement between experiment and CDW calculation. We have refrained from applying this correction to the data of figure 1 since the polarisation of the  $\text{He}^+(n=4 \rightarrow n=2)$  transition is not known.

### 3.2. Proton-argon collisions

The H(2p) alignment in proton-argon collisions shows similar features if compared with the helium data. They in addition display a pronounced maximum below 1 keV (figure 4). As for the helium target, H(2p) excitation in proton-argon collisions at low incident velocities is the result of a two-step process, populating first the ground-state charge exchange channel, followed by a radial or rotational coupling to the  $4p\sigma$  or  $3d\pi$  mo, respectively (Sidis 1972, Hippler *et al* 1985). The pronounced maximum below 1 keV indicates that at low incident energies  $\pi$ -state excitation is dominant.

In figure 4, a few data for deuteron impact are also presented. To facilitate comparison with the proton data, the kinetic energy was divided in this figure by the projectile mass. It follows from comparison of the proton and deuteron data that the integral alignment scales satisfactorily with the projectile velocity.

A final remark should be made concerning the influence of cascading transitions originating from the population of higher H( $nl$ ) states (e.g. H( $n=3,1$ )) on the present observations. Measurements of Ford and Thomas (1972) for protons on helium show for example that between 100 and 300 keV the cross section for H(3s) production is roughly three times as large as that for H(2p) production. (This result is incidently confirmed by our CDW calculations.) However, the H(3s) state has a lifetime  $\tau_{3s} = 158$  ns  $\approx 100 \tau_{2p}$ , corresponding to a flight path of about 0.7 m at 100 keV. Therefore, although capture to the 3s state will be sizeable, their decay will take place almost exclusively outside the observation region of length 2.5 cm (see, e.g., Wolterbeek Muller and de Heer 1970, Hippler *et al* 1978). The 3d states are also not expected to influence

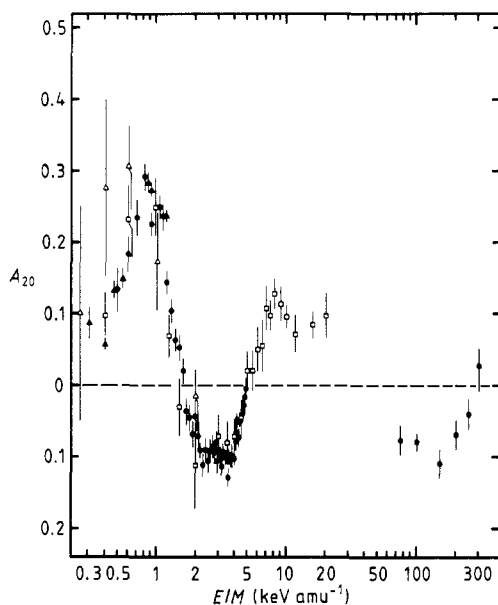


**Figure 4.** Integrated alignment  $A_{20}$  plotted against incident proton energy for  $H^+$ -Ar and  $D^+$ -Ar collisions. Proton impact:  $\bullet$ , present data;  $\square$ , Teubner *et al* (1970); deuteron impact:  $\blacktriangle$ , present data;  $\triangle$ , Teubner *et al* (1970).

the present results since, as recently determined by Tepperwien *et al* (1985), the initial population of H(3d) is 3–5 times smaller than that of H(2p) with  $\tau_{3d} = 15 \text{ ns} \approx 10 \tau_{2p}$ . Any other cascading transition will have an even smaller influence due to the smaller corresponding cross section and longer lifetime.

#### 4. Conclusions

The measured integral alignment  $A_{20}$  of H(2p) excitation in  $H^+$ -He, Ar collisions displays a pronounced dependence on the incident proton energy. At low energies H(2p) charge exchange excitation is the result of a two-step process. Two-electron unified AO-MO calculations of Kimura and Lin (1985) are here in excellent agreement with experiment for  $H^+$ -He collisions, and up to proton energies of 80 keV. The agreement with theory is less satisfactory for proton energies of 100 keV or greater, where the experimental data are compared with CDW calculations.

#### Acknowledgments

The authors acknowledge helpful discussions with Professor Hans Kleinpoppen, Dr J Burgdörfer, Dr M Kimura, Professor C D Lin and J Bossler.

This work was supported by the Deutsche Forschungsgemeinschaft in SFB 216 'Polarisation und Korrelation in atomaren Stoßkomplexen'.

**References**

- Andreev E P, Ankudinov V A and Bobashev S V 1966 *Sov.-JETP* **23** 375-82
- Burgdörfer J 1981 *Phys. Rev. A* **24** 1756-67
- Burgdörfer J and Dubé L J 1984 *Phys. Rev. Lett.* **52** 2225-8
- Clarke D and Grainger J F 1971 *Polarized Light and Optical Measurement* (Oxford: Pergamon)
- Cheshire I M 1964 *Proc. Phys. Soc.* **84** 89-98
- CRC Handbook of Chemistry and Physics* 1979 (Boca Raton, Florida: CRC)
- Dose V 1966 *Helv. Phys. Acta* **39** 683-6
- Dubé L J 1984 *J. Phys. B: At. Mol. Phys.* **17** 641-58
- Fano U and Macek J 1973 *Rev. Mod. Phys.* **45** 553
- Ford J C and Thomas E W 1972 *Phys. Rev. A* **5** 1694-701
- Hasselkamp D, Hippler R, Scharmann A and Schartner K H 1971 *Z. Phys.* **248** 254-63
- Hippler R 1985 *Fundamental Processes in Atomic Collision Physics* ed H Kleinpoppen, J S Briggs and H O Lutz (New York: Plenum) p 181-213
- Hippler R, Faust M, Wolf R, Kleinpoppen H and Lutz H O 1985 *Phys. Rev. A* **31** 1399-404
- Hippler R, Schartner K-H and Beyer H F 1978 *J. Phys. B: At. Mol. Phys.* **11** L337-41
- Hughes R H, Stigers C A, Doughty B M and Stokes E D 1970 *Phys. Rev. A* **1** 1424-32
- Kimura M and Lin C D 1985 private communication and to be published
- Macek J 1984 *Proc. 13th Int. Conf. on Physics of Electronic and Atomic Collisions* ed J Eichler, I V Hertel and N Stolterfoht (Amsterdam: North-Holland) Invited paper pp 317-30
- Macek J and Jaecks D H 1971 *Phys. Rev. A* **4** 2288
- Moustafa Moussa H R and de Heer F J 1967 *Physica* **36** 646-54
- Pretzer D, van Zyl B and Geballe R 1964 *Proc. 3rd Int. Conf. on Physics of Electronic and Atomic Collisions (London) 1963* (Amsterdam: North-Holland) p 618
- Sidis V 1972 *J. Phys. B: At. Mol. Phys.* **5** 1517-28
- Tepperwien W, Bruch R, Dubé L and Zuccatti S 1985 *Nucl. Instrum. Meth. B* **10/11** 198-203
- Teubner P J O, Kauppila W E, Fite W L and Girmius R J 1970 *Phys. Rev. A* **2** 1763-7
- Thomas E W 1972 *Excitation in Heavy Particle Collisions* (New York: Wiley-Interscience)
- Thomas E W and Bent G D 1967 *Phys. Rev.* **164** 143-50
- Wolterbeek Muller L and de Heer F J 1970 *Physica* **48** 345-96